Robust Optical FFH-CDMA Communications: Coding in Place of Frequency and Temperature Controls

Habib Fathallah, *Student Member, IEEE,* and Leslie A. Rusch, *Member, IEEE*

***Abstract*— In wavelength division multiplexing (WDM), transmitters require stringent and complex frequency control loops to avoid wavelength drifts due to temperature fluctuations. This makes the transmitters heavy, bulky, and inappropriate for local- and short-haul communications networks, as well as for manufacturing locales and other open areas where temperature control is not feasible. We propose and analyze a technique we call robust fast frequency hopping code division multiple access (FFH-CDMA), particularly suitable for severe, hostile, noncontrollable environments. This approach avoids all conditioning and frequency stabilization loops in the transmission end. We develop a modified version of extended hyperbolic congruence codes to achieve environment-resistant codes. We present expressions for the auto- and cross-correlation functions for optical implementation of the codes. We simulate the encoding/decoding operations with parameters from real Bragg gratings. We evaluate probability of error for a single user and as an average over all users versus capacity (the number of simultaneous users). Robust FFH-CDMA is an efficient access technique for hostile environments. It avoids the frequency and temperature control problems of WDM and nonrobust FFH-CDMA [1]–[3] at the cost of lower overall capacity in terms of number of simultaneous users.**

***Index Terms*— Bragg grating, optical fast frequency hopping code division multiple access (FFH-CDMA), wavelength control and lasers stabilization in WDM, wavelength division multiplexing (WDM).**

I. Introduction

In wavelength division multiplexing (WDM), optical sources must transmit at precise, distinct wavelengths. Temperature fluctuations at a transmitter can lead to significant wavelength drift. Stringent frequency control loops and complex tracking systems are required to avoid this drift [7]–[8], involving optic-to-electronic and electronic-to-optic conversion devices. The result is heavy, cumbersome transmitters that are unsuitable for local area networks (LAN's), fiber-to-home access networks, short-haul interconnecting and multiplexing, on-board naval and avionics communications, and manufacturing locales and other open areas where temperature control is not feasible.

To avoid frequency stabilization we employ coded communications, in particular code division multiple access (CDMA). In direct sequence CDMA a cyclic pattern of ± 1 (called the code sequence) is imprinted on the data in the time domain. At the receiver a copy of this sequence is correlated with the received signal. If the correct cycle of the sequence is applied, the portion of the received signal coded with this sequence is decoded. The code is chosen to have a clearly discernable autocorrelation peak, so that the receiver can cycle in time through the sequence to achieve synchronization with the transmitted code. In frequency-hopped CDMA the coding is done in two dimensions: time and frequency. Each bit interval is parsed in time (into chip intervals) and a certain frequency is transmitted during each chip. The decoding operation recombines the signal that during coding was distributed across the time and frequency domains. During traditional FFH-CDMA, the two-dimensional (2-D) code is translated only in the time dimension to achieve synchronization. Typically an absolute frequency reference is assumed, i.e., frequency synchronicity, so that translation over the frequency domain is not necessary. In radio frequency (RF) frequency-hopped CDMA, Doppler shift can corrupt the frequency reference so that the decoder must seek the autocorrelation peak while shifting over both the time and frequency domains.

In optical communications there is no Doppler shift, however, frequency drift of source lasers due to environmental affects, especially temperature fluctuations, has a similar effect. Robust Frequency-hopped CDMA allows communications despite frequency drift, therefore obviating frequency-stabilization routines. In this paper we propose such a system and address two major concerns: 1) an encoding/decoding device which can easily perform the correlation while shifting the code (or hop pattern) over both the time and frequency domain and 2) codes which have the necessary autocorrelation peak over two dimensions and that also conform to the physical constraints of the coding device.

The system proposed is robust to environmental effects that can be modeled as nonfrequency selective; whenever the environmental effect has the same behavior at each frequency in the communications band, communications are possible despite the frequency drift. Bragg gratings (BG) and several BG based devices such as distributed feedback (DFB) lasers exhibit nonfrequency selective drift. The encoding–decoding

Manuscript received September 25, 1998; revised April 21, 1999. This work was supported by a grant from the natural Sciences and Engineering Research Council of Canada and by QuébécTel. This paper was presented in part at the Eleventh Tyrrhenian International Workshop on Digital Communications, "The Optical Network Layer: Management, Systems, and Technologies," Portofino, Italy, September 1999.

The authors are with COPL, the Department of Electrical and Computer Engineering, Laval University, P.Q. G1K 7P4 Canada (e-mail: fhabib@gel.ulaval.ca).

Publisher Item Identifier S 0733-8724(99)06346-X.

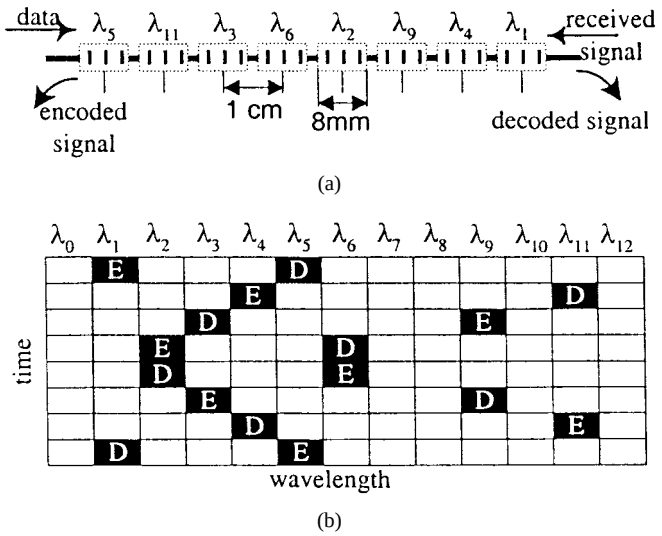

Fig. 1. (a) FFH-CDMA encoder/decoder based on multiple Bragg gratings and (b) frequency-hop pattern of the encoder (respectively, the decoder): the mark E (respectively D) marks the encoder (respectively the decoder) pulses.

device proposed in [1]–[2], recently demonstrated in [3], produced in Fig. 1(a), for fast frequency hopping-code division multiple access (FFH-CDMA) is based on BG, and therefore has nonfrequency selective drift. In [1], the transmitters of the optical CDMA communications system are stabilized to the environment parameters' fluctuations. In contrast, the version proposed here is called robust FFH-CDMA, as we avoid stabilization and frequency control loops, at the cost of decreased overall capacity in terms of number of users.

In Section II, we discus the frequency drift problem and control complexity in WDM systems. In Section III, we explain how BG exhibit nonfrequency selective drift. The basic mathematical formalism of the robust optical FFH-CDMA system is presented in Section IV. The environmental effect on the FFH-CDMA signal, in cases of BG and DFB lasers based encoders, are discussed in Section V. In Section VI, we propose a robust FFH-CDM system architecture, derive suitable environment-resistant codes, simulate the encoding–decoding operations using real Bragg gratings parameters, calculate the system maximum capacity in terms of number of users and we evaluate the probability of error both in mean and for a single user.

II. Frequency Drift in WDM

In DWDM (Dense Wavelength Division Multiplexing) communications, each wavelength is dedicated to one independent transmitter–receiver pair. The wavelengths coincide with a predetermined grid, fixing their values and spacing. The ITU standard fixes the wavelengths to a spacing of 100 GHz [4], [8]. In such systems, each transmitter must generate a very precise wavelength. Physical characteristics of the optical devices in the transmission end, especially source lasers, can lead to wavelength drift due to environmental fluctuations, especially changes in ambient temperature. One obvious solution is the absolute control of semiconductor laser wavelengths for WDM applications.

A. Distributed Grating-Based Lasers

For telecommunication systems, the most commonly used laser sources are distributed feedback (DFB) or distributed Bragg reflector (DBR) lasers [6]–[8]. This is due to their highly monomode spectrum where the emission frequency is set by the selective reflectivity of the distributed grating. When the ambient temperature changes, the distributed grating characteristics change and hence the emission frequency of the laser changes. Two parameters are usually used to control the frequency of a semiconductor laser, the junction temperature and the injection current. In Section III, we further address the temperature dependency of the DFB laser frequency.

Temperature fluctuations affect not only source lasers, but any Bragg grating devices. Gratings are widely used in communications for filtering, multiplexing, waveform shaping and encoding–decoding and channel equalization. The performance of these devices is also sensitive to the ambient temperature variation and requires stringent control of their environment.

B. Frequency Control Problem

One popular way to stabilize the frequency of a laser source is to lock it to a stable optical reference. High precision is usually obtained using an atomic or molecular transition as an optical reference in the transmitter. Many atomic and molecular transitions are available at both 1.3 and 1.55 μm, which are usually observed using optogalvanic detection or optical pumping techniques [8]. These frequency stabilization techniques are typically very complex and require a stringent control of environmental parameters at each transmission site. Control loops require additional optic-to-electronic and electronic-to-optic conversion devices, making the transmitter heavy and cumbersome.

While a surmountable impediment for long-haul communications, the complexity and bulk of frequency stabilization has limited the success of WDM for LAN's, fiber-to-home access networks, short-haul communications, security and surveillance systems, on-board naval and avionics communications. In these applications, we must: 1) reduce the system bulk and weight, 2) avoid environmental conditioning, and 3) reduce system complexity, especially the number of active devices. The last requirement is critical to ensure system reliability.

III. Nonfrequency Selective Environmental Effects

As an alternative to frequency control techniques we propose a coded communications system that is robust to environmental effects that can be modeled as nonfrequency selective. Whenever the environmental effect has the same behavior at each frequency within the communications band in use, i.e., nonfrequency selective, communications is possible despite frequency drift. There are several devices, which exhibit nonfrequency selective drift. Our approach is predicated on having a broad-band source and encoding–decoding devices (see Section V) with nonfrequency selective drift. Bragg gratings can be modeled as having by nonfrequency selective drift in their reflectivity. DFB lasers based on Bragg gratings also have this property. In order to insure that source frequency

drift is independent of operating frequency, the source must not undergo any mode-hopping in response to environmental effects. For this reason Fabry–Perot lasers would not make suitable sources.

A. Bragg Gratings

Fiber Bragg gratings, usually produced by exposure of photosensitive fiber to ultraviolet light, have a refractive index that is spatially periodic along the fiber propagation axis. The Bragg grating operates as an optical band-pass (or band stop) filter centered at the so-called Bragg wavelength given by the expression $\lambda_B = 2n_{\text{eff}}\Lambda$, where Λ is the grating period and n_{eff} is the effective index of the core. The Bragg grating wavelength is particularly sensitive to two parameters: strain and temperature, which are usually used to tune Bragg gratings and also makes them attractive devices for fiber-based sensors. While our results apply equally to drift due to strain, temperature variations are most common, and in this paper we refer only to temperature affects.

The wavelength shift due to temperature variation ΔT is

$$\Delta\lambda_B = [(dn_{\text{eff}}/dT)/n_{\text{eff}} + (d\Lambda/dT)/\Lambda]\lambda_B \Delta T \qquad (1)$$

where the first term arises from the temperature dependency of the refractive index, and the second term is due to the thermal expansion of the fiber. The former is dominant and accounts for about $\sim$95% of the total shift. Experimental observations show that [5]

$$\frac{\Delta\lambda_B}{\lambda_B} = 6.67 \times 10^{-6}\Delta T \qquad (2)$$

for the communications band. This equation indicates that wavelength shift $\Delta\lambda_B$ is frequency selective, i.e., the constant of proportionality between $\Delta\lambda_B$ and ΔT is frequency dependent. However, in practice, the wavelength drift is much narrower than the wavelength itself, ($\sim$30 nm in the 1550 nm band), and therefore we can approximate $\Delta\lambda_B = 6.67 \times 10^{-6} \times 1550 \times \Delta T$.

B. DFB Lasers

The operating wavelength of a distributed feedback (DFB) laser is determined by the etched grating through the Bragg wavelength given by $\lambda_B = 2\bar{\mu}\Lambda/m$, where $\bar{\mu}$ is the mode index, Λ is the grating period, and m is the diffraction order of the grating. Therefore DFB lasers have the same temperature dependence as Bragg gratings. In our analysis of an environmentally resistant FFH technique, we assume that no mode hops can occur in the transmission. This is a reasonable assumption for DFB lasers as the built-in grating provides high stability of the longitudinal mode over a wide range of temperature (20–108 °C reported in [5]). The wavelength of a DFB laser changes with temperature at a rate $\Delta\lambda_B/\Delta T \cong 01$ nm/°C without mode hopping. In [6], it was recently demonstrated that DFB lasers designed from erbium doped fiber also present a stable longitudinal and polarization single-mode operation without mode hopping in a range of temperature as wide as (−196 to 200 °C). Fabry–Perot lasers are generally less stable than DFB lasers and frequently exhibit mode jumps with the temperature variation.

IV. Optical FFH-CDM

The proposed coded robust communications system employs techniques borrowed from CDMA. In this section we introduce the standard mathematical formalism used to model a CDMA system and to evaluate its performance. We adapt this formalism to our particular system of 2-D codes, and we derive modified expressions for the signal-to-noise ratio and probability of error.

A. Time and Frequency Domain Characteristics

In FFH-CDM system, the information bits are encoded with 2-D matrix codes simultaneously exploiting the time and frequency domains. The matrix codes are chosen to be as transparent (or mathematically orthogonal) as possible. We use codes adopted for RF FFH-CDMA as a starting point for our analysis. These codes have their transparency optimized to combat two affects: time domain asynchroncity (i.e., user transmissions have a random relative delay modeled with a uniform distribution) and frequency domain Doppler shift (due to relative motion of transmitter and receiver). Temperature-induced frequency drift in optical systems will have characteristics different from those of Doppler-shifted RF communications, and therefore the codes used will be suboptimal. In order to assess the performance of these codes via the signal-to-interference ratio (SIR) and bit error rate (BER) (discussed later in Section IV.D) we will average over the distribution of the temperature variation.

B. Encoding and Decoding

In an optical FFH system, each data bit is multiplied by a waveform called an FFH code or sequence. This waveform is a concatenation of the so-called *chip pulses*, each of which occupies a distinct frequency slot and is transmitted in a distinct *chip* time slot of duration T_c. The FFH sequence can be mathematically expressed as

$$c_k(t) = \sum_{j=1}^{N} d_{k,j}\psi_j(t - jT_c) \qquad (3)$$

where N is the length of the code (or the number of chips per bit), $d_{k,j} \in \{0, 1\}$, for $1 \le j \le N$, is the jth chip value of the kth user's code, T_c is the chip duration and $T = NT_c$ is the bit duration. The chip signaling waveform $\psi_j(t)$, for $1 \le j \le N$, is usually assumed to be rectangular with unit energy. In an FFH encoding technique based on multiple Bragg gratings, $\psi_j(t)$ is the time-convolution of the incident data-modulated, wideband, noncoherent short pulse with the jth single grating impulse response. The impulse response of a single grating is defined in this paper as the inverse Fourier transform of the grating complex reflectivity.

In [1], we assumed that the data pulse is much narrower than the impulse response duration. However in [3], an experimental demonstration of the standard FFH-CDMA system shows that the impulse responses of actual gratings are much narrower than data modulated 300 ps pulses. The gratings introduce very little expansion of the incident pulse. Such gratings can be modeled as a train of Dirac delta

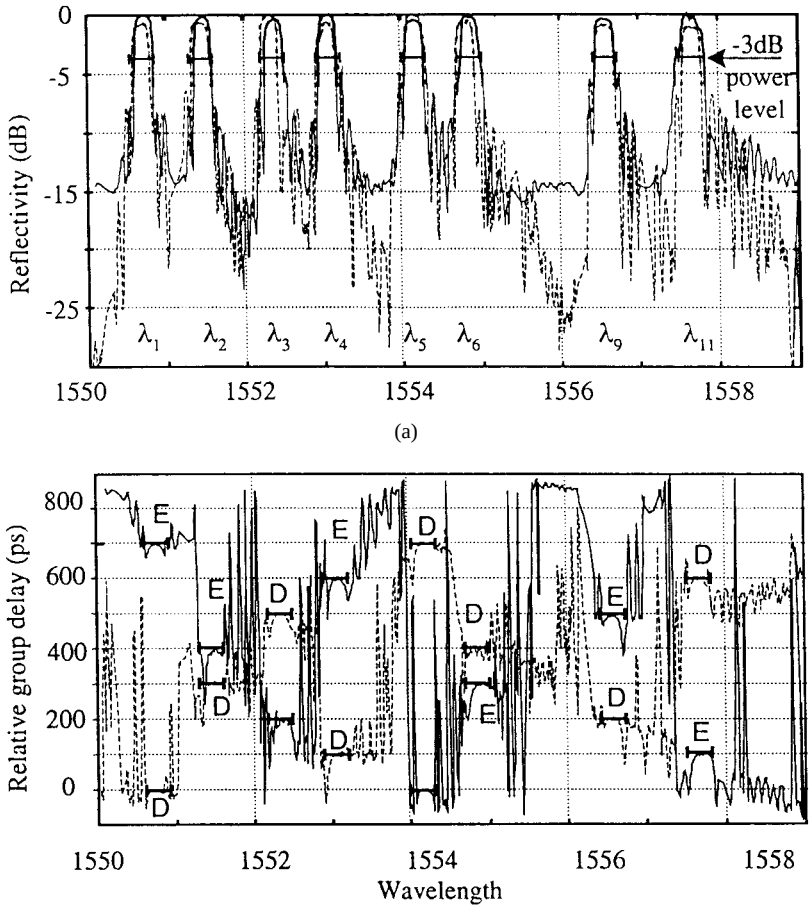

Fig. 2. (a) Reflected spectrum from the encoder (solid line) and the decoder (dotted line) and (b) the group delay for each frequency bin of the encoder (solid line) and of the decoder (dotted line). The marks E and D have the same meaning as in Fig. 1.

functions when compared to data pulses lasting hundreds of picoseconds.

Since we assume noncoherent source is used and with on/off data modulation, the system is entirely positive. The decoding operation at the receiver consists of a power-summation, i.e., square law detection and comparison of the recombined pulses with a constant threshold. The phase spectra of the gratings, therefore, need not add coherently. Fig. 2(a) and (b) reports real measured characteristics of one standard FFH-CDMA encoder/decoder pair [3], where an eight-wavelength multiple Bragg grating is written in a fiber segment of length 8 cm. Each grating is of length 8 mm and spacing between cascaded gratings is 2 mm, as described in Fig. 1(a).

We introduce a special notation to express the sensitivity of the FFH code to environment temperature. Let c_k^{α} be the transmitted FFH sequence at the temperature $T_\alpha = T_0 + \alpha\Delta T$, where T_0 is an arbitrary nominal temperature, ΔT is the amount of temperature variation which can change the transmitted wavelength by one increment, B_0, i.e., one frequency slot, and α a coefficient which quantifies the temperature variation in the system. While in practice temperature variation will be continuous and not in discrete steps, we present a discrete form of our analysis for heuristic reasons only. The results apply equally to continuous temperature variation for ambient temperature. The temperature-shifted code pulse is therefore

$$\mathbf{c}_k^{\alpha}(\mathbf{t}) = \sum_{j=1}^{N} \mathbf{d}_{k,j}\psi_j^{\alpha}(\mathbf{t} - \mathbf{jTc}) \tag{4}$$

where $\psi_j^{\alpha}(\mathbf{t})$ is the jth chip pulse whose center frequency will be shifted for $T_\alpha \neq T_0$.

In a robust FFH-CDM system each user k, for $k = 1, \ldots, K$, transmits a sequence c_k^{α} corresponding to its own temperature T_{α_k}. At the receiver, the received signal is a sum of all the transmitted signals

$$r(t) = \sum_{k=1}^{K} b_k c_k^{\alpha_k}(t - \tau_k) \tag{5}$$

where $b_k \in \{0, 1\}$ is the kth user information bit during the bit interval $(0, T)$, τ_k is the time delay of user k with $0 \leq \tau_k \leq T_c$ and α_k is the temperature variation coefficient of user k. We assume each time delay is constant and uniformly distributed over a bit interval. The receiver applies a matched filter to the incoming signal to extract the desired user's bit stream. For notational simplicity, we assume that the desired user's signal is denoted by $k = 1$, $\tau_1 = 0$. The matched filter output for

bit interval $(0,T)$ is thus

$$y = \int_0^T c_1^0(t) r(t)\,dt = \int_0^T c_1^0(t) c_1^{\alpha_1}(t)\,dt + \sum_{k=2}^{K} b_k \int_0^T c_1^0(t) c_k^{\alpha_k}(t-\tau_k)\,dt \quad (6)$$

where we have neglected the effects of quantum noise and thermal noise. The first term in (6) corresponds to the desired user, the second is multiple access interference (MAI). Ideally, the users' codes should be mutually orthogonal (or transparent), leading to MAI equal to zero and the receiver output y will be only the desired user contribution. When the temperature of the desired user's environment shifts from the nominal temperature T_0, the coefficient $\alpha_1 \neq 0$, i.e., $c_1^0(t)$, the locally generated desired user's code, $c_1^0(t)$ is spectrally shifted with respect to the transmitted code. In an ideal system, the first term is zero when the locally generated code $c_1^0(t)$ does not match $c_1^{\alpha_1}(t)$, i.e., the code should be orthogonal (or transparent) to any frequency shifted version of itself. Assuming that tuning of the matched filter from $c_1^0(t)$ to $c_1^{\alpha_1}(t)$ is accomplished by exploiting an auto-correlation peak of the code described in the next section, the receiver output becomes

$$y = \int_0^T c_1^{\alpha_1}(t) r(t)\,dt = \int_0^T \left(c_1^{\alpha_1}(t)\right)^2 dt + \sum_{k=2}^{K} b_k \int_0^T c_1^{\alpha_1}(t) c_k^{\alpha_k}(t-\tau_k)\,dt = b_1 N + \mathrm{MAI} \quad (7)$$

In most CDM systems, the MAI is the most important noise source. For a large number of multiplexed signals, the probability density function of the MAI is usually approximated to be Gaussian, appealing to central limit theorem arguments. To reduce the effect of the MAI, codes with specific transparency characteristics are required, especially codes that remain orthogonal (or almost-orthogonal) even under frequency and time shift.

C. Auto- and Cross Correlation

A convenient way for representing an FFH code is by use of a placement operator (or frequency hop pattern), i.e., a sequence of N ordered integers determining the placement of frequencies in the N available time slots. Each user selects a set of N frequencies from a sets of q available frequencies $\mathbf{S} = \{f_1, f_2 \ldots, f_q\}$, where $N \leq q$. The frequency-hop pattern is usually represented by a matrix $(N \times q)$ showing the time and frequency plane.

Most codes developed for radio FFH-CDMA assume $N = q$. Only a few code families can be generalized to $N < q$; all are suboptimal. In our system the number N is determined by the complexity of the encoder (see Section V-A). The number of available frequencies q is limited by the expected maximum variation of the environmental parameters (discussed further in Section VI). Codes used in other optical FFH-CDMA systems [12], [13] are not appropriate, as frequency shifts lead to high correlation among codes. In this system, as described in Section VI-B, we modify square $(N = q)$ extended hyperbolic congruence codes, already resistant to RF Doppler shift, for this robust FFH-CDMA system. The codes used are one-coincidence sequences, i.e., 1) all of the sequences are of the same length, 2) in each sequence, each frequency is used at most once, and 3) the maximum number of hits between any pair of sequences for any time shift equals one [9], [10]. These parameters are usually measured using the so-called auto- and cross-correlation functions defined in the following.

Let $c_k(i,j)$ be the frequency-hop pattern of user k when the time slot is i and the frequency slot is j. Therefore $c_k(i,j)$ is one if there is a transmission for user k in time slot $1 \leq i \leq N$ and frequency slot $1 \leq j \leq q$; otherwise it is zero. Let

$$\Omega_1 = \left|\min_k \alpha_k\right| \quad \Omega_2 = \max_k \alpha_k.$$

Each code in the code family should be selected to maximize the peak and minimize the sidelobes of the autocorrelation function over all delays τ and frequency shifts s

$$R_m(\tau,s) = \sum_{j=0}^{q}\sum_{i=0}^{N} \mathbf{c}_m(i,j)\mathbf{c}_m(i-\tau, j-s) \quad \text{where } -N+1 \leq \tau \leq N-1 \quad \text{and} \quad -\Omega_1 + 1 \leq s \leq \Omega_2 - 1 \quad (8)$$

where ideal auto-correlation corresponds to $R_m(0,0) = N$, the number of ones in the code (or the weight of the code) and $R_m(\tau,s) = 0$ otherwise. Secondly, the cross-correlation should be minimized for all pairs of codes c_m and c_n in the code family for all delays τ and frequency shifts s

$$R_{m,n}(\tau,s) = \sum_{j=0}^{q}\sum_{i=0}^{N} \mathbf{c}_m(i,j)\mathbf{c}_n(i-\tau, j-s) \quad \text{where } -N+1 \leq \tau \leq N-1 \quad \text{and} \quad -\Omega_1 + 1 \leq s \leq \Omega_2 - 1 \quad (9)$$

where ideal cross-correlation corresponds to $R_{m,n}(\tau,s) = 0$ for all time and frequency shifts. Note that cross-correlation term is visible in the MAI portion of the matched filter output in (6). Ideal auto- and cross-correlation functions are difficult to acheive in realistic CDMA systems. We exploit codes having good, though not ideal, auto- and cross-correlation properties.

D. SIR and Probability of Error

To evaluate the signal to interference ratio at the receiver output we require the probability density function of the time-shift (or delay) as well as that of the frequency-shift between any users. We consider a system where all users transmit without time synchrony. The probability density function (pdf) of the random time delay is well modeled as uniform over a bit duration. A uniform density is not however, necessarily a good model for the *pdf* of the temperature-induced frequency

shift. Let Π be the discrete probability density function of the frequency-shift s so that

$$\Pi(s) = \text{Prob}(\textit{frequency shift} = s) \quad \text{and} \quad \sum_{s=\Omega_1+1}^{\Omega_2-1} \Pi(s) = 1. \tag{10}$$

In a real system, the *pdf* can be estimated using statistical analysis of the parameters influencing environmental fluctuations.

Let $\bar{R}_{m,n}$ be the cross-correlation averaged over delay and frequency-shift between codes m and n. Since the time-shift and the frequency-shift are independent variables we arrive at

$$\bar{R}_{m,n} = \frac{1}{2N-1} \sum_{s=-\Omega_1+1}^{\Omega_2-1} \Pi(s) \sum_{\tau=-N+1}^{N-1} R_{m,n}(\tau, s). \tag{11}$$

The variance of the cross-correlation between codes m and n is

$$\sigma_{m,n}^2 = \frac{1}{2N-1} \sum_{s=-\Omega_1+1}^{\Omega_2-1} \Pi(s) \sum_{\tau=-N+1}^{N-1} (R_{m,n}(\tau, s) - \bar{R}_{m,n})^2 \tag{12}$$

Since we do not know which codes will be active at any given time, we further average over all code pairs to arrive at $\sigma^2 = \mathbf{E}\{\sigma_{m,n}^2\}$ where $\mathbf{E}$ indicates the expected value over uniformly distributed indices m and n. With these definitions, the mean value of the MAI for K active users can be expressed as $\mu_{\text{MAI}} = (K-1)\bar{R}_{m,n}$. Assuming the interfering users are statistically independent, the MAI has variance that can be approximated as

$$\sigma_{\text{MAI}}^2 = (K-1)\sigma^2. \tag{13}$$

The signal to interference can then be easily derived as

$$\text{SIR} = N^2/(K-1)\sigma^2. \tag{14}$$

The output of the matched filter is compared to the threshold $\eta = N/2 + \mu_{\text{MAI}}$ to decide if a bit was transmitted. Using the Gaussian assumption for the MAI, and assuming the system is MAI limited (i.e. neglecting other noise sources) the probability of error for equiprobable data is given by

$$\begin{aligned} P_e &= \text{Prob}(y \geq \eta \mid b_1 = 0) \cdot \text{Prob}(b_1 = 0) \\ &\quad + \text{Prob}(y \leq \eta \mid b_1 = 1) \cdot \text{Prob}(b_1 = 1) \\ &= \frac{1}{2}\{\text{Prob}(y \geq \eta \mid b_1 = 0) + \text{Prob}(y \leq \eta \mid b_1 = 1)\} \\ &= Q(N/\sqrt{(K-1)\sigma^2}) = Q(\sqrt{\text{SIR}}) \end{aligned} \tag{15}$$

where $Q(x) = \frac{1}{\sqrt{2\pi}} \int_x^{+\infty} e^{\frac{-u^2}{2}}\, du$.

V. Encoding–Decoding Devices

As explained in Section III, Bragg gratings can be modeled as having nonfrequency selective drift in their reflectivity. Furthermore, fiber Bragg gratings are a key component in several optical devices, especially DFB laser sources, which are widely used in telecommunications due to their monomode output, stability and simplicity. In this section, we present two possible FFH-encoding techniques and explain the environmental effect on the FFH signal.

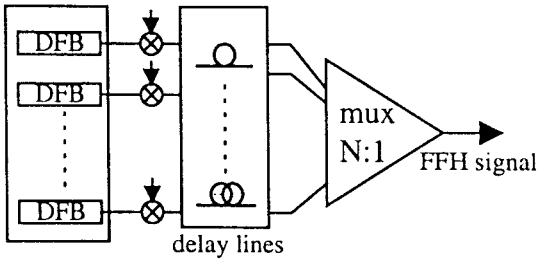

Fig. 3. DFB array-based FFH-CDMA encoder.

A. Bragg Gratings

In [1]–[3], the FFH-CDMA waveform is passively applied to the data modulated signal via multiple fiber Bragg gratings. As shown in Fig. 1(a), we propagate the data modulated short pulses along the multiple Bragg gratings which imprints its impulse response onto the signal. The grating frequencies are selected and the gratings are physically placed along the fiber in the order prescribed by the frequency-hop pattern [see Fig. 1(b)]. The round trip propagation time between two gratings should correspond to a chip interval T_c. Let L_c be the sum of one grating length and one spacing distance between adjacent grating pairs, let c be the speed of light, let n_{eff} be the average value of the effective refractive index; and let n_g be the effective group index; then $T_c = 2n_gL_c/c$. Therefore the total round trip time in a grating structure of N Bragg gratings is given by $2(N-1)L_cn_0/c$, effectively determining the minimum bit duration T. Fig. 2(a) and (b) shows, respectively, experimentally measured reflectivity and delay time of a fiber multiple Bragg gratings written to the FFH code $(\lambda_5, \lambda_{11}, \lambda_3, \lambda_6, \lambda_2, \lambda_9, \lambda_4, \lambda_1)$ using the physical parameters specified in Fig. 1(a). Recall that $L_c = 10$ mm, i.e., $T_c = 100$ ps and $T = 800$ ps.

When all gratings are written for high-coupling coefficient, leading to very high reflectivity (>95%) their wavelengths can not be reflected more than one time as all significant energy at this wavelength is reflected by the first occuring grating. This means that for the in-line structure of the proposed multiple Bragg gratings, no frequency can be used more than one time. Furthermore, it is actually difficult to superpose gratings with predictable characteristics, therefore, no more than one frequency can be used at once. These physical properties coincide with those of one coincidence sequences defined primarily in Section IV-C.

At the receiver, similar multiple Bragg gratings programmed in the reverse order as the encoder will compensate the relative delays between the pulses received from the desired user the dotted line curves in Fig. 2(a) and (b) presents the decoder reflectivity and time delay. The pulses from the desired user will superpose in a peak, while the pulses from an interfering user will contribute to background noise as quantified by the cross-correlation.

As described in Fig. 3, an array of DFB lasers can be used to generate the multiwavelength signal. All wavelengths are simultaneously modulated to generate the chip pulses, each of which is passed through an appropriate delay line as prescribed by the code. All the chip pulses are summed using a standard

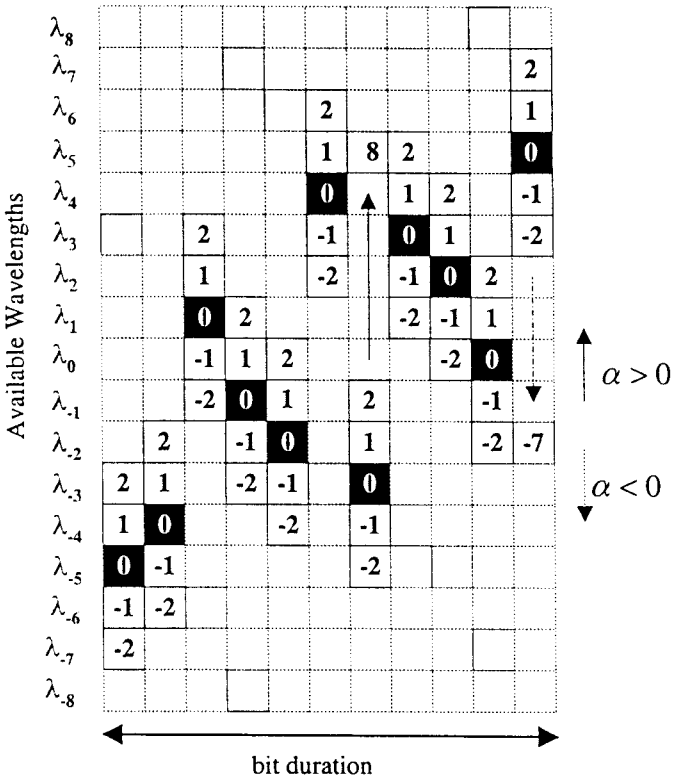

Fig. 4. Temperature variation effect on FFH-CDMA signal.

optical WDM multiplexer. This FFH waveform generation process is clearly less interesting than one based on Bragg gratings, because it requires a high number of devices leading to high-power loss. Other FFH-encoding techniques can be designed using a combination of spectral slicing and delay lines. Switching and/or tunability can be used to perform programmable FFH encoding.

B. Environmental Effects on the FFH Signal

When the temperature of one FFH transmitter increases, all wavelengths of the transmitted FFH signal simultaneously and identically increase, i.e., nonfrequency selective drift. As mentioned in Section II.B), the Bragg grating wavelength shift actually depends on the Bragg wavelength, but the restricted region of interest (30 nm in the 1550 nm region) makes nonfrequency selective drift a reasonable assumption. For the DFB based FFH encoder, it should be assumed that no mode hopping occurs when the temperature shifts.

If the spectrum of the data modulated wideband signal is large and flat enough, the total transmitted energy does not change with the ambient temperature variation. In effect, the number of transmitted pulses and their energy do not change. An example of an FFH encoded signal is shown in Fig. 4, with code $\mathbf{w}_0 = [\lambda_{-5}\,\lambda_{-4}\,\lambda_1\,\lambda_{-1}\,\lambda_{-2}\,\lambda_4\,\lambda_{-3}\,\lambda_3\,\lambda_2\,\lambda_0\,\lambda_5]$ at the initial ambient transmitter temperature T_0 (which corresponds to the squares marked by 0). Let ΔT be the positive temperature change corresponding to a wavelength drift of one increment B_0, i.e., the temperature causing λ_k to drift to λ_{k+1}. When the ambient temperature changes with an amount equal to α times ΔT becoming $T_\alpha = T_0 + \alpha\Delta T$ the effectively transmitted sequence will be $\mathbf{w}_\alpha = [\lambda_{-5+\alpha}\,\lambda_{-4+\alpha}\,\lambda_{1+\alpha}\,\lambda_{-1+\alpha}\,\lambda_{-2+\alpha}\,\lambda_{4+\alpha}\,\lambda_{-3+\alpha}\,\lambda_{3+\alpha}\,\lambda_{2+\alpha}\,\lambda_{\alpha}\,\lambda_{5+\alpha}]$. Let $\mathbf{I}$ be a vector of $N-1$ components ($N-1=10$ in the example of Fig. 4) describing the wavelength subscript increment in the code.

$$\mathbf{I}_k(i) = \text{subscript}(\mathbf{u}_k(i+1)) - \text{subscript}(\mathbf{u}_k(i)).$$

For example, the first component of $\mathbf{I}$ equals the second wavelength subscript of the code minus the first wavelength subscript. For $\mathbf{w}_0$, we calculate $\mathbf{I} = [1\ 5\ -2\ -1\ 6\ -7\ 6\ -1\ -2\ 5]$. Since $\mathbf{w}_\alpha$ is a simple frequency shift of $\mathbf{w}_0$, they have identical increment vector $\mathbf{I}$. This means that the temperature variation changes the wavelengths but not the increment vector $\mathbf{I}$. Note that the increment vector is a placement operator of length $N-1$.

In our system where transmitters are not temperature-stabilized, the increment vector of the frequency FFH code is sufficient to decode the message. The receiver starts with a decoder programmed for the desired user (that is for the correct increment vector) and tuned to a nominal set of frequencies corresponding to the nominal temperature T_0. The receiver tunes the decoder gratings in unison (i.e., maintaining the same increment vector) and searches for an auto-correlation peak. In Section VI, we simulate the temperature effect on the transmitted code, present the 2-D (time and temperature) autocorrelation function and we show that the capacity of this multiplexing system is reduced compared to the optical FFH-CDMA with a stabilized environment.

We addressed Bragg gratings and DFB lasers as examples of encoding–decoding devices to combat the effect of the environment on the FFH-signal, however, it is important to note that the robustness property of the system is inherent to the FFH communications technique itself and any encoding devices having nonfrequency selective drift can be used.

VI. Robust FFH-CDM System Performance

In Fig. 5, we show a robust FFH-CDM system based on multiple Bragg gratings and composed of one programmable receiver and K transmitters. A broad-band source and a rapid external modulator (at the chip-rate or lower) can be shared amoung all the users or a subgroup of users to generate a stream of broad-band short pulses (chip-duration). Each transmitter uses its own low rate (bit rate) external modulator to insert its data sequence into the incoming short pulses, and its fixed multiple Bragg gratings to insert its own code.

A. Processing Gain

The processing gain PG is a critical integer parameter for every CDMA system, as it quantifies the resources shared between users via the codes. The higher the PG, the higher the number of available codes and the greater the ease of discriminating among users. In FFH-CDM, the PG for a code family expressed as

$$\text{PG} = (\text{number of available frequency slots}) \times (\text{number of available times slots})$$

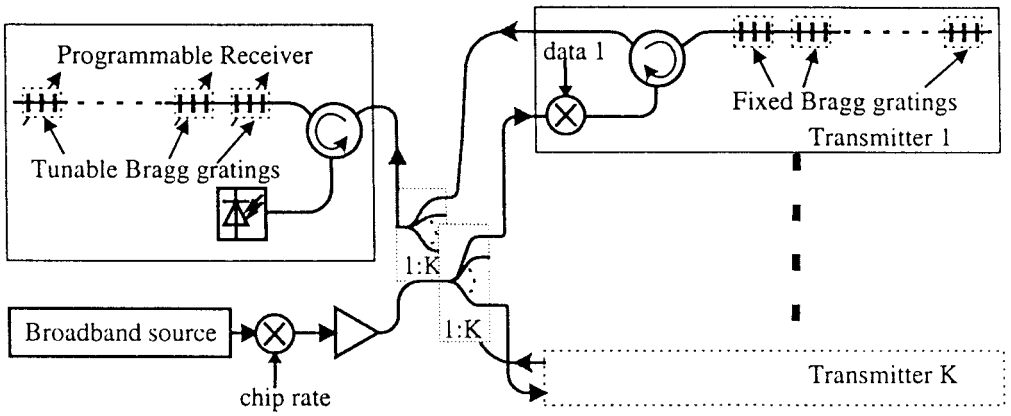

Fig. 5. Proposed robust FFH-CDM communications system.

where the number of frequencies available for occupation in the system is limited by 1) the bandwidth of the source and 2) grating tuning bandwidth. The number of time slots is limited by the number of gratings. Since the combination of fiber stretching (up to 7 nm) and compression (up to 30 nm) leads to very wide range of tunability in the system, we consider that the source bandwidth is the limiting factor for determining the number of available wavelengths. In temperature stabilized optical FFH-CDMA, the entire source bandwidth (BW) can be used for encoding, however this robust FFH-CDMA system requires upper and lower guard bands (each with bandwidth GB) to accommodate frequency drifts due to environmental effects. This results in a decrease in the number of frequency slots q, hence a reduction of the processing gain and the reduced capacity as compared to previously proposed FFH-CDMA. The number of frequency slots is reduced per

$$q_0 = \frac{\mathrm{BW}}{B_0} \quad \text{versus} \quad q = \frac{\mathrm{BW} - 2\mathrm{GB}}{B_0}$$

where B_0 is the combined bandwidth of the frequency slot and spacing between slots.

B. Derivation of Codes

The encoding space is rectangular (N time slots $< q$ frequency slots), however, most RF FFH-codes assume $N = q$. In [11], the authors developed a new family of codes called extended hyperbolic codes (EHC) which have good auto- and cross-correlation properties under simultaneous frequency and time shift. The EHC placement operator can be expressed as

$$y_{i,m}(k) \equiv \begin{cases} 1/(ik+m) \bmod(p) & \text{if } ik \neq -m \bmod(p) \\ 0 & \text{if } ik = -m \bmod(p) \end{cases} \tag{16}$$

where, p is a prime number (for our system $p = q$), $k = 1, \ldots, q-1$ is the number of chip time slots, i is the user number and $m = 0, \ldots, q-1$ is the so called message number. For this application we can select $m = 0$ and consequently reduce the cross-correlation between codes. While the EHC codes are not rectangular codes, they can be adapted to our needs. Since the $q \times q$ codes satisfy the required auto- and cross-correlation properties, any truncated codes of size $q \times N$ will also have the same properties.

While the EHC codes in [11] offer good performance for frequency shifts from $-q$ to q, our system has shifts constrained by the guard bands (by construction the guard bands represent maximal frequency variation). Therefore our codes need to be efficient for shifts equal to

$$-(q_0 - q)/2 \leq s \leq (q_0 - q)/2.$$

We therefore propose the following modified EHC codes:

$$y_{i,0}(k) \equiv \begin{cases} 1/(ik) \bmod(q) & \text{if } k \neq 0 \bmod(q) \\ 0 & \text{if } k = 0 \bmod(q) \end{cases}$$
$$\text{for } i = 1, \ldots, N-1; \quad k = 0, 1, \ldots, N-1. \tag{17}$$

This derives $q-1$ different modified (or truncated) extended hyperbolic codes (TEHC), each of which uses N frequencies among the available q. It should be noted that the TEHC have performance at least as good as the EHC codes, however, they remain suboptimal.

C. Illustrative Example

A superfluorescent source (SFS) can provide a signal of 30 nm bandwidth centered at the wavelength 1550 nm. Using the same Bragg gratings physical parameters and wavelength spacing as in [1], we achieve up to $q_0 = 135$ available disjoint frequency slices taking into account the adequate spacing between slots. In the time domain, a fiber of 20 cm length supports 12 gratings for a data rate of 500 MB/s. To match the OC 12 standard (622 MB/s), a shorter length of 16 cm is assumed here for 12 gratings without significant overlap between chip pulses (physical spacing between gratings being reduced from 8 mm to 4 mm). With these parameters a temperature stabilized FFH-CDMA has PG $= q_0 \times N = 135 \times 12 = 1620$.

In order to determine the guard bands required we assume $T_0 = 0$°C to be the maximal temperature and 4 nm to be the maximum wavelength increase and/or decrease expected due to temperature fluctuations. In [1], the fiber DFB lasers presented high linearity in a temperature range as wide as ~400 °C in the interval (−196 ° to 200°C), which leads to a frequency shift of ~4 nm. This means that remaining bandwidth for encoding is $(30 - 2 \times 4) = 22$ nm corresponding to ~99 wavelengths. For ease of code generation, we select

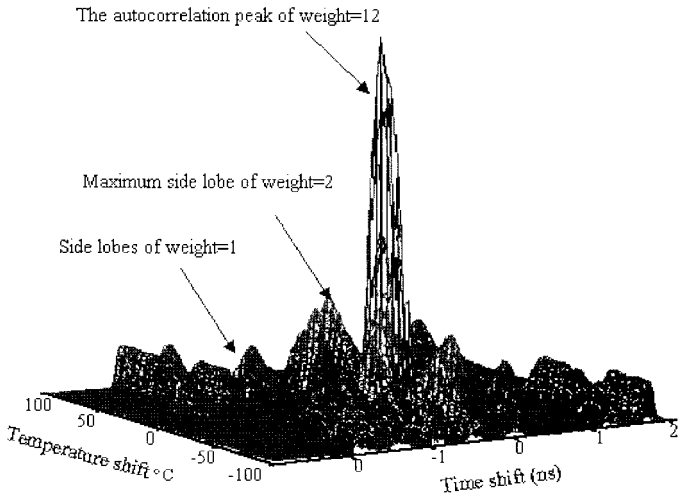

Fig. 6. Two-dimensional (time and temperature shifts) autocorrelation function.

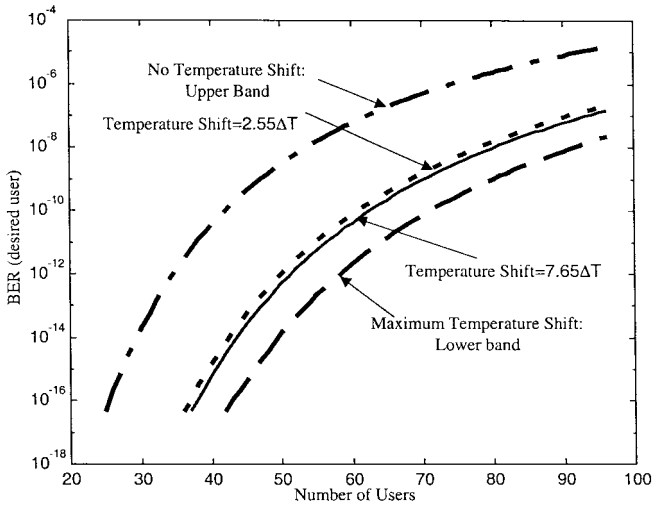

Fig. 7. Average probability of error versus capacity.

the prime number $q = 97$ as the effective available number of wavelengths to be shared among the robust FFH-CDMA system. The processing gain of the robust FFH-CDMA is consequently

$$\text{PG} = (\text{number of frequency slots} = 97) \times (\text{number of times slots} = 12) = 1164$$

D. Simulation Results: Autocorrelation Function

In this section, we simulate two 12 frequency multiple Bragg gratings using the parameters of the previous illustrative example in the previous section. To avoid long simulation time we restricted the number of available frequencies to $q = 17$. We derived the TEHC's as described in Section VI-B. We simulated ambient temperature variation of -100 to $+100$ °C in 5 °C steps. This includes, for example, the range of ambient winter temperature in Québec City, where temperatures can be lower than -60 °C in open areas, and where it can exceed 30 °C in enclosed areas. Fig. 6 shows that the correlation between an encoder maintained at nominal initial temperature of 0 °C and a decoder searching through all possible temperature and time delays. We use a high central peak (weight 12) when the decoder temperature is 0 °C and time synchronization is achieved. Otherwise, the correlation leads to sidelobes with maximum weight of two.

E. Probability of Error

To evaluate the system performance in terms of probability of error we assume a Gaussian *pdf* for the temperature, with mean T_0 and standard deviation η. The temperature of each transmitter is assumed to be independent and identically distributed. Simulations use parameters from the previous section and TEHC codes described in Section VI-B. In the following we evaluate the probability of error of the system averaged over all users, as well as the probability of error of a single user. We present the probability of error as a function of the number of active users, for various values of η. Recall ΔT is the temperature shift leading to frequency drift B_0.

1) Average Probability of Error Versus Capacity: In Fig. 7, we present the average probability of error of the proposed robust communications system as a function of the number of users. The curves clearly show that the higher the number of active transmitters, the higher the probability of error. This is obviously due to the increase MAI interference. It is important to note that the environment stabilized FFH-CDMA system gives an upper bound [curve (a)] to the probability of error in the system. Stabilization of the transmitters keeps all users' signals in the central frequency band and out of the guard bands, which leads to greater cross-correlation between users and higher MAI. On the other hand, a uniform distribution of the frequency shift gives a lower bound to the probability of error [curve (d)], as drifted codes tend to cover the entire available bandwidth. Curves (b) and (c) correspond respectively to a temperature shift *pdf* with $\eta = 2.55 \times \Delta T$ and $\eta = 7.65 \times \Delta T$. As can be expected, decreasing η leads to increasing MAI and a degradation of the average probability of error. Fig. 5 shows that for probability of error of 10^{-9} the system can accommodate $\approx$45 simultaneous users in a temperature-stable scenario, and 74 simultaneous users when the temperature is uniformly distributed.

2) Single Probability of Error Versus Capacity: Suppose that one transmitter exhibits a frequency shift, therefore pulses from its signal are present in a guard band. This reduces its coincidence probability with the interferers, i.e., reduces the MAI, and consequently improves its probability of error. Fig. 8 shows the single user probability of error versus the number of users depending on the frequency shift of the desired user. An unchanged temperature shift gives an upper bound to the probability of error since the variance of the MAI is the highest. When the transmitter exhibits the maximum frequency shift the single probability of error achieves its lower bound since the MAI is at its lowest.

VII. Conclusion

We propose a new optical multiple access communications technique which is robust to environmental fluctuations and

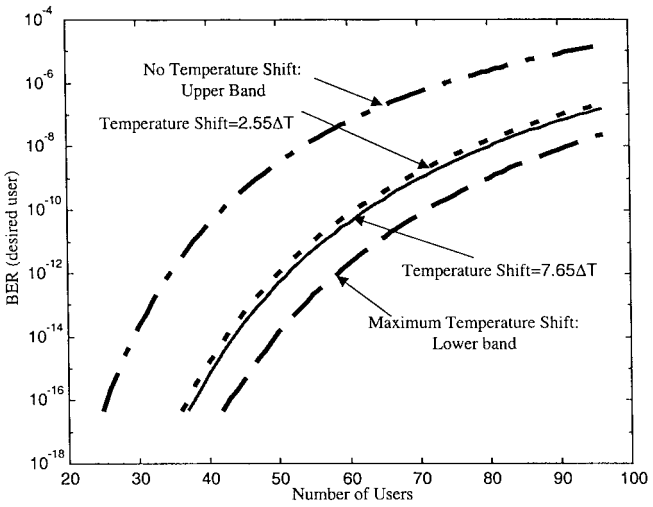

Fig. 8. Single probability of error versus capacity.

avoids any stabilization or conditioning of the transmitters. We analyze the technique we call robust FFH-CDMA. We develop a modified version of extended hyperbolic congruence codes to achieve environment-resistant codes. We derive modified expressions of the auto- and cross-correlation functions.

The simplicity of the proposed robust communications system makes it suitable for local area networks (LAN's), fiber-to-home access networks, short-haul communications, security and surveillance systems, on-board naval and avionics communications. In such applications, the complexity and bulk of frequency stabilization of the transmitters has limited the success of WDM. The robust FFH-CDMA system avoids the stabilization problems of WDM and nonrobust FFH-CDMA [1] at the cost of lower overall capacity. We evaluate the processing gain of robust versus nonrobust FFH-CDMA. Simulation shows that for probability of error of 10^{-9} the system can accommodate 45–74 simultaneous users depending on probability density function of the temperature shift.

REFERENCES

[1] H. Fathallah, L. A. Rusch, and S. LaRochelle, "Passive optical fast frequency-hop CDMA communications system," *J. Lightwave Technol.*, vol. 17, pp. 397–405, Mar. 1999.

[2] H. Fathallah, L. A. Rusch, and S. LaRochelle, "Fast frequency hopping spread spectrum for code division multiple access communications networks (FFH-CDMA)," U.S. Pat. Pend., June 1998.

[3] H. Fathallah, P.-Y. Cortès, L. A. Rusch, S. LaRochelle, and L. Pujol, "Experimental demonstration of an optical fast frequency hopping-CDMA communications system," to appear in *ECOC'99*, Sept. 1999.

[4] International Telecommunication Union, Telecommunication Standardization Sector, Study Group 15, Question 25, Recommendation G.mcs, 1996.

[5] A. D. Kersey, "A review of recent developments in fiber optic sensor technology," *Opt. Fiber Technol.*, vol. 2, pp. 291–317, 1996.

[6] P. Varming, J. Hübner, and M. Kristensen, "Five wavelength DFB fiber laser source," in *Proc. Tech. Dig. Opt. Fiber Commun.*, 1997, pp. 31–32.

[7] T. Ikegami, S. Sudo, and Y. Sakai, *Frequency Stabilization of Semiconductor Laser Diodes*. Boston, MA: Artech House, 1995.

[8] M. Guy, B. Villeneuve, C. Latrasse, and M. Têtu, "Simultaneous absolute frequency control of laser transmitters in both 1.3 and 1.55 μm bands for multiwavelength communication systems," *J. Lightwave Technol.*, vol. 14, pp. 1136–1143, June 1996.

[9] L. Bin, "One-coincidence sequences with specified distance between adjacent symbols of frequency-hopping multiple access," *IEEE Trans. Commun.*, vol. 45, pp. 408–410, Apr. 1997.

[10] S. V. Maric and E. L. Titlebaum, "A class of frequency hop codes with nearly ideal characteristics for use in multiple-access spread-spectrum communications and radar and sonar systems," *IEEE Trans. Commun.*, vol., pp. 1442–1447, 1992.

[11] L. D. Wronski, R. Hossain, and A. Albicki, "Extended hyperbolic congruential frequency hop code: Generation and bounds for cross- and auto-ambiguity function," *IEEE Trans. Commun.*, vol. 44, pp. 301–305, Apr. 1996.

[12] H. Fathallah, L. A. Rusch, and S. LaRochelle, "Optical frequency-hop multiple access communications system," in *Proc. 1998 IEEE Int. Conf. Commun.*, Atlanta, GA, June 1998, paper 36-2.

[13] H. Fathallah, S. LaRochelle, and L. A. Rusch, "Analysis of an optical frequency-hop encoder using strain-tuned Bragg gratings," in *Proc. OSA Topical Meeting on Bragg Gratings, Photosensitivity, and Poling in Glass Fibers and Waveguides: Applications and Fundamentals*, Oct. 1997, pp. 200–202.

Habib Fathallah (S'96), for photograph and biography, see p. 405 of the March 1999 issue of this JOURNAL.

Leslie A. Rusch (S'91–M'94), for photograph and biography, see p. 405 of the March 1999 issue of this JOURNAL.